FISEVIER

Contents lists available at ScienceDirect

The Lancet Regional Health - Western Pacific

journal homepage: www.elsevier.com/locate/lanwpc



Research paper

Meteorological conditions and nonpharmaceutical interventions jointly determined local transmissibility of COVID-19 in 41 Chinese cities: A retrospective observational study

Li-Qun Fang^{a,1}, Hai-Yang Zhang^{a,1}, Han Zhao^{b,1}, Tian-Le Che^{a,1}, An-Ran Zhang^{a,c,d}, Ming-Jin Liu^c, Wen-Qiang Shi^a, Jian-Ping Guo^e, Yong Zhang^b, Wei Liu^{a,*}, Yang Yang^{c,*}

- ^a State Key Laboratory of Pathogen and Biosecurity, Beijing Institute of Microbiology and Epidemiology, Beijing, PR China
- ^b School of Mathematical Sciences, Beijing Normal University, Beijing 100875, PR China
- Department of Biostatistics, College of Public Health and Health Professions, and Emerging Pathogens Institute, University of Florida, Gainesville, FL, USA
- ^d Department of Epidemiology, School of Public Health, Shandong University, Jinan, PR China
- ^e The State Key Laboratory of Severe Weather, Chinese Academy of Meteorological Sciences, Beijing 100081, PR China

ARTICLE INFO

Article history: Received 12 July 2020 Revised 11 August 2020 Accepted 25 August 2020

ABSTRACT

Background: Before effective vaccines become widely available, sufficient understanding of the impacts of climate, human movement and non-pharmaceutical interventions on the transmissibility of COVID-19 is needed but still lacking.

Methods: We collected by crowdsourcing a database of 11 003 COVID-19 cases from 305 cities outside Hubei Province from December 31, 2019 to April 27, 2020. We estimated the daily effective reproduction numbers (R_t) of COVID-19 in 41 cities where the crowdsourced case data are comparable to the official surveillance data. The impacts of meteorological variables, human movement indices and nonpharmaceutical emergency responses on R_t were evaluated with generalized estimation equation models.

Findings: The median R_t was 0•46 (IQR: 0•37–0•87) in the northern cities, higher than 0•20 (IQR: 0•09–0•52) in the southern cities (p=0•004). A higher local transmissibility of COVID-19 was associated with a low temperature, a relative humidity near 70–75%, and higher intracity and intercity human movement. An increase in temperature from 0°C to 20°C would reduce R_t by 30% (95 CI 10–46%). A further increase to 30°C would result in another 17% (95% CI 5–27%) reduction. An increase in relative humidity from 40% to 75% would raise the transmissibility by 47% (95% CI 9–97%), but a further increase to 90% would reduce the transmissibility by 12% (95% CI 4–19%). The decrease in intracity human movement as a part of the highest-level emergency response in China reduced the transmissibility by 36% (95% CI 27–44%), compared to 5% (95% CI 1–9%) for restricting intercity transport. Other nonpharmaceutical interventions further reduced R_t by 39% (95% CI 31–47%).

Interpretation: Climate can affect the transmission of COVID-19 where effective interventions are implemented. Restrictions on intracity human movement may be needed in places where other nonpharmaceutical interventions are unable to mitigate local transmission.

Funding: China Mega-Project on Infectious Disease Prevention; U.S. National Institutes of Health and National Science Foundation.

© 2020 The Author(s). Published by Elsevier Ltd.

This is an open access article under the CC BY-NC-ND license.

(http://creativecommons.org/licenses/by-nc-nd/4.0/)

Introduction

The first wave of the coronavirus disease 2019 (COVID-19) had been largely controlled in China by mid-April, after massive implementation of stringent nonpharmaceutical interventions including movement restrictions, social distancing, wearing face masks, case isolation, and contact tracing and quarantine [1]. Epidemics outside

^{*} Corresponding authors.

E-mail addresses: liuwei@bmi.ac.cn (W. Liu), yangyang@ufl.edu (Y. Yang).

 $^{^{1}}$ These authors contributed equally.

Hubei Province in the country were characterized by inefficient local transmission and low case fatality rates, owing to swift and comprehensive public health responses immediately following the lockdown of Wuhan [2]. By the end of April, most cities (92•3%) had lowered the level of public health response and shifted focus to the prevention of disease importation and resurgence.

The wide time lag in epidemic curves between northern hemisphere and southern hemisphere countries has raised the question about the role of seasonality in the pandemic of SARS-CoV-2, the causative virus for COVID-19. A few recent studies on the impacts of climatic factors on the spread of COVID-19 found negative associations of disease incidence with temperature and humidity, while others found none [3–6]. Two studies associated the effective reproduction numbers (R_t) in China with climatic factors, yet both ignored two important facts: (1) a large proportion of cases were imported from Wuhan; and (2) crowdsourced data are incomplete for most cities in China [4,6]. Two modeling studies assessed the role of seasonality in future global transmission dynamics of SARS-CoV-2, but the seasonality was derived from other human coronaviruses or influenza [7,8].

Human movement is a key driver for the diffusion of infectious agents [9]. Several early studies found that the implemented intercity travel restrictions had little effect in delaying the spread of COVID-19 from Wuhan to other cities in China, and two of these studies showed a beneficial impact of suspending intracity public transport [1,10,11]. In additional to travel restrictions, other typical nonpharmaceutical interventions such as social distancing and case finding and isolation were also effective in curbing the epidemics in China and other countries, either alone or in combination [1,11-13]. None of these studies explicitly presented reduction in the reproduction number due to human movement restrictions which is more generalizable than reduction in case incidence, especially in the presence of case importation. In addition, climatic conditions might have affected both human movement and transmissibility of the disease and therefore should be controlled for when one evaluates the effects of human movement restrictions on transmissibil-

Using crowdsourced data of cases and case clusters in 305 cities of China, we summarized the epidemiological features of COVID-19 outside Hubei Province. We estimated city-specific real-time effective reproduction numbers and examined how climatic indices, intercity and intracity human movement, and other public health emergency responses jointly shaped the R_t dynamics in 41 cities of China where our data are nearly as complete as the officially reported COVID-19 cases in the national surveillance system. Finally, we predicted potential R_t values in these cities throughout the year of 2020 under different levels of control, in particular to answer the question whether it is safe to lift the intracity human movement restrictions while maintaining other nonpharmaceutical interventions.

Methods

Sources of data

COVID-19 cases and associated transmission clusters were mainly obtained by crowdsourcing (Appendix p 1–3). The primary data sources are websites and social media accounts of local health commissions and branches of the Chinese Center for Disease Prevention and Control (China CDC). For possible additional information, we also searched internet using keywords in the form of ("coronavirus" OR "pneumonia") AND (province or city names), all in Chinese. For each identified COVID-19 case, basic demographic characteristics (age, sex, and city), starting and ending dates of probable exposure, date of symptom onset, laboratory diagnosis status, and associated epidemiological cluster were retrieved if

available. Cases reported in Hubei Province were excluded due to lack of individual information in the public domain. To provide robust estimation of R_t , we then cross-checked the number of cases by city, age, sex and symptom onset date (or reporting date if symptom onset date is not available) with the national surveillance data provided by China CDC, and identified 41 cities satisfying the following inclusion criteria: (1) the crowdsourced data cover ≥85% of surveillance-reported cases; and (2) case clustering information and whether each case was imported or locally infected are known (Appendix p 10 and 20). These criteria are necessary for reliable assessment of R_t and its drivers. Data from these 41 cities were analyzed for the primary analysis. The surveillance data from China CDC were not directly usable for estimating local transmissibility due to lack of case clustering and case importation information. The timelines of nonpharmaceutical intervention measures implemented by municipal governments and level-1 emergency responses initiated by provincial governments were collected from governmental websites and news media (Appendix p 23-25).

Daily ambient temperature and relative humidity (RH) during January and February of 2020 were collected from the Chinese Academy of Meteorological Sciences. Weather station readings were interpolated to the cities by krigging. Daily average PM_{2.5} data were obtained from open weather forecast websites (http://106.37.208.233:20035). Population densities were collected from the National Bureau of Statistics of China (www.stats.gov.cn). Daily intercity migration data (immigration index) and the daily values of an urban traffic index reflecting ground transportation activities in each city during 2019 (Jan 12–Mar 13) and 2020 (Jan 1–Feb 27) were obtained from the open website of Baidu Corporation (http://qianxi.baidu.com/).

This study was approved by the institutional review board (IRB) of the Beijing Institute of Microbiology and Epidemiology (Beijing, China). All the case data had been deidentified before they were made publicly accessible by public health authorities. All analyses directly involving individual-level dates were performed at the Beijing Institute of Microbiology and Epidemiology.

Statistical analyses

Descriptive analysis and estimating natural history of disease

Pearson's Chi-square test was performed to compare categorical variables between groups, and Wilcoxon rank sum test and Kruskal-Wallis test were used to compare continuous variables between groups. To estimate the distribution of the incubation period, cases with onset dates and probable exposure period observed were used (Appendix p 3-4). Exposure was determined by either recent residence in or travel to Wuhan or an epidemiological link with a potential source case who had either an earlier symptom onset or recent residence in or travel to Wuhan. Cases with either the starting or the ending exposure dates missing or with an exposure ≥15 days were excluded. The log-rank test adjusted for interval-censoring was used to compare incubation periods between groups. To estimate the serial intervals, we identify transmission pairs of primary cases and their potential secondary cases from clusters of epidemiologically linked cases. In such a pair, both cases had symptom onset dates, but only the primary case had lived in or traveled to Wuhan or had a clear evidence of contacting an earlier confirmed case. We fitted parametric models using lognormal, gamma, log-logistic and Weibull distributions, and the best fitted model was determined by the Akaike's Information Criterion.

Estimating R_t and associated determinants A COVID-19 patient is defined as an imported case if he or she had residence in or travel history to Hubei Province (where Wuhan is located) during the 2 weeks before symptom onset or as a local case otherwise.

Referring to the earliest symptom onset date in each case cluster as day 0, we define a primary case as either a local case with symptom onset on days 0 or 1 or an imported case with symptom onset on days 0–3. Other cases were considered secondary cases. A cluster may have multiple co-primary cases. Coupling these definitions, the confirmed cases were partitioned into four categories: imported primary cases, imported secondary cases, local primary cases, and local secondary cases, which were defined in our previous study [14]. We used a simple moving average approach to estimate the effective reproduction number R_t for each day within the study period (Appendix p 4–5) [14]. Briefly, the general estimator for R_t is given by

$$\hat{R}_{t} = \frac{N_{sec}(t-2,t+2)}{N_{pri}(t-2,\,t+2) + \tilde{N}_{sec}(t-2,t+2)},$$

where $N_{pri}(t_1,t_2)$ and $\tilde{N}_{sec}(t_1,t_2)$ are the total numbers of primary and secondary cases, respectively, in all clusters whose onset dates were within the time window $[t_1,t_2]$, and $N_{sec}(t_1,t_2)$ is the total number of secondary cases who might have been infected during the same window. In the primary analysis, all imported cases, including imported secondary cases, are considered as primary cases (infectors) and contribute to $N_{pri}(t-2, t+2)$. The numerator, $N_{sec}(t-2, t+2)$, includes local secondary cases whose primary cases in the same cluster had symptom onset during [t-2, t+2], as well as local primary cases whose infection likely occurred in this interval. A sensitivity analysis was conducted by treating imported secondary cases as infectees rather than infectors.

To assess potential selection bias in the 41 cities chosen for the primary analysis, we identified additional nine cities with \geq 70% coverage of surveillance-reported cases and complete information on case importation. We then combined the nine cities with the 41 cities for another sensitivity analysis. As case-clustering information is not available for the nine cities, we applied a traditional approach for calculating R_t that ignores case-clustering (Appendix p 6) [15].We adapted this approach to account for imported cases.

Based on the estimated R_t values in each city, we then used a generalized estimation equation (GEE) model to assess the impacts of seven potential risk factors on daily R_t : air temperature, relative humidity, PM_{2.5}, immigration index, traffic index, population density, and an indicator for the time period of implementation of nonpharmaceutical interventions (Appendix p 6-8) [16]. All factors are time-dependent except for population density. Selection of polynomial orders and optimal time lags was based on the Quasilikelihood under Independence Model Criterion (QIC) [17]. To account for the temporal correlation of the R_t values in each city, we assumed an autoregressive correlation structure of order 1 that induces a decreasing correlation for further apart time points, which is justified by the partial autoregressive correlations of estimated R_t series in selected cities (Appendix p 13). A backward procedure based on both p-values and QIC was used for model selection. The model was fitted using the R package "geepack". Using the final model, we predicted weekly R_t values in the 41 cities throughout 2020 under a variety of intervention assumptions.

Role of the funding source

The funder of the study had no role in study design, data collection, data analyses, interpretation of the results, or the writing of the manuscript. The corresponding authors had full access to all the data and had final responsibility for the decision to submit for publication.

Results

By crowdsourcing, we collected individual-level demographic, exposure and disease information on 11 003 laboratory-confirmed

cases, including 1360 clusters (≥2 cases per cluster), from 305 cities outside Hubei Province, whose symptom onsets span from Dec 31, 2019 to Apr 27, 2020. These cases account for 84•2 % of and share a similar temporal trend with the 13 069 cases outside Hubei Province who were reported by China CDC for the same period, excluding cases imported from abroad (Appendix p 11).

Among the 11 003 cases, 83•7% were adults aged 15–64 years, 12•7% were the elderly over 65 years, and the remaining 3•6% were children 0–14 years (Table 1). There were more male cases (52•1%) than female cases (47•9%). More cases were reported in southern China (45•8%). The dominant type of known infection source was household contact (56•8%), followed by dining out (17•3%). The CFR was 0•9% among cases whose final survival outcome are known. Imported cases were slightly younger than local cases, and primary cases were less likely to be children (<15 years old) and elderlies (≥65 years old) than secondary cases. Among cases whose final clinical outcomes are known, local cases had a higher CFR (1•1%) than imported cases (0•6%).

We estimated the median incubation period to be 6.06 (95% CI: 5.84-6.29 days), and 5th and 95th percentiles to be 1.74 and 12.21 days respectively (Appendix p 22). The duration of the incubation period was not associated with sex, region, clinical outcome or cluster size. The median incubation period was about 1 day longer among children <15 years old compared to older cases (p=0.02) and was slightly longer after the initiation of level-1 emergency response compared to before (p=0.01, Appendix p 12 and 22). Using 648 pairs of cases for whom the transmission relationship is relatively clear, we estimated a median serial interval of 4.8 days (95% CI 4•4-5•3 days) (Appendix p 22). The serial interval tended to be longer when the infector was a male vs. a female (median=5.3 vs. 4.4 days, p=0.01) and when the infector was a local case vs. an imported case (median=6.7 vs. 3.5 days, p<0.001). In contrast to the incubation period, the serial interval contracted after the initiation of level-1 emergency response (p=0.06, Appendix p 12 and

In the 41 cities where the crowdsourced data are relatively complete, a total of 4 431 COVID-19 cases, including 1965 imported cases, contributed to the analysis of R_t and associated determinants. The daily volume of passengers departing Wuhan increased sharply during the Chunyun (spring festival commute) period starting around Jan 7, topped at nearly 80 000 persons on Jan 21, and dropped dramatically on and after Jan 23 when the lockdown of Wuhan began (Fig. 1A). The number of symptom onsets among infected travelers to the 41 cities grew exponentially from 7 on Jan 13 to 154 on Jan 24 and declined rapidly afterwards. Cities at higher latitudes were associated with later importation and epidemic peaks. Shenzhen and Guangzhou, both in the South, had the largest total numbers and peak daily numbers of cases, followed by Xinyang in central China and Harbin in the North (Fig. 1B-C). More migrant cases went to the southern cities than to the northern cities (Fig. 1C; Table 1).

We estimated the daily effective reproduction numbers, R_t , for each region as well as for each of the 41 cities. The overall trends of the R_t values over time are similar across regions (Fig. 2), starting at nearly 2 in middle January and quickly descending to below the critical value of 1 by Jan 24 in the northern region, Jan 22 in the central region and Jan 20 in the southern region. The median region-level R_t was 0.46 (IQR: 0.37–0.87) in the northern region, similar to 0.40 (IQR: 0.14–0.76) in the central region (p=0.22) but higher than 0.20 (IQR: 0.09–0.52) in the southern region (p=0.004). The city-specific trends of R_t mostly resemble those at the regional level, although there appeared to be more variations especially when the number of cases was small (Appendix p 14–16). The median city-level R_t dropped from 1.0 (IQR: 0.7–1.7) one week before the initiation of level-1 responses to 0.6 (IQR: 0.4–0.9) one week after. In addition, eight out of 15 south-

Table 1 Characteristics of crowdsourced COVID-19 patients as of April 27, 2020 in 305 cities of mainland China.

Characteristics	Category	All cases	Imported	Local	p-value [‡]	Primary	Secondary	<i>p</i> -value [‡]
Age, year	0-14	369 (3•6)	166 (4•0)	203 (3•3)	<0•0001	194 (2•4)	175 (8•1)	<0•0001
	15-64	8 560 (83•7)	3 604 (87•9)	4 956 (80•9)		6 930 (85•9)	1 630 (75•6)	
	65-97	1 296 (12•7)	331 (8•1)	965 (15•8)		944 (11•7)	352 (16•3)	
	Unknown	778	203	575		697	81	
Sex	Male	5 615 (52•1)	2 375 (56•4)	3 240 (49•3)	<0.0001	4 576 (53•5)	1 039 (46•8)	<0.0001
	Female	5 164 (47•9)	1 835 (43•6)	3 329 (50•7)		3 984 (46•5)	1 180 (53•2)	
	Unknown	224	94	130		205	19	
Location [†]	Northern China	2 190 (19•9)	634 (14•7)	1 556 (23•2)	<0.0001	1 511 (17•2)	679 (30•3)	<0.0001
	Central China	3 777 (34•3)	1 426 (33•1)	2 351 (35•1)		3 044 (34•7)	733 (32•8)	
	Southern China	5 036 (45•8)	2 244 (52•1)	2 792 (41•7)		4 210 (48•0)	826 (36•9)	
Infection	Household contact	2 082 (56•8)	289 (54•3)	1 793 (57•2)	<0.0001	959 (48•5)	1 123 (66•5)	<0.0001
source								
	Dining out	635 (17•3)	44 (8•3)	591 (18•9)		366 (18•5)	269 (15•9)	
	Public places	364 (9•9)	18 (3•4)	346 (11•0)		249 (12•6)	115 (6•8)	
	Hospitals	200 (5•5)	12 (2•3)	188 (6•0)		98 (5•0)	102 (6•0)	
	Work places	119 (3•2)	33 (6•2)	86 (2•7)		94 (4•7)	25 (14•8)	
	Public transportation	266 (7•3)	136 (25•5)	130 (4•2)		212 (10•7)	54 (3•2)	
	Unknown	3 870	0	3 870		3519	351	
Level-1	Before	2 490 (22•6)	1 566 (36•4)	924 (13•8)	<0.0001	2 340 (26•7)	150 (6•7)	<0.0001
emergence	After	8 513 (77•4)	2 738 (63•6)	5 775 (86•2)		6 425 (73•3)	2 088 (93•3)	
Castrome	Discharge	9 686 (99•1) (99•2)	3 979 (99•4)	5 707 (98•9)	0.0051	7 747 (99•1)	1 939 (99•0)	0.8580
	Death	89 (0•9)	23 (0•6)	66 (1•1)		70 (0•9)	19 (1•0)	
	Unknown	1 228	302	926		948	280	
Total		11 003	4 304	6 699		8 765	2 238	

 $^{^\}dagger$ Including 111, 70, 124 cities from northern, central, and southern China, respectively.

 $^{^{\}ddagger}$ p-values are based on Pearson's Chi-square test.

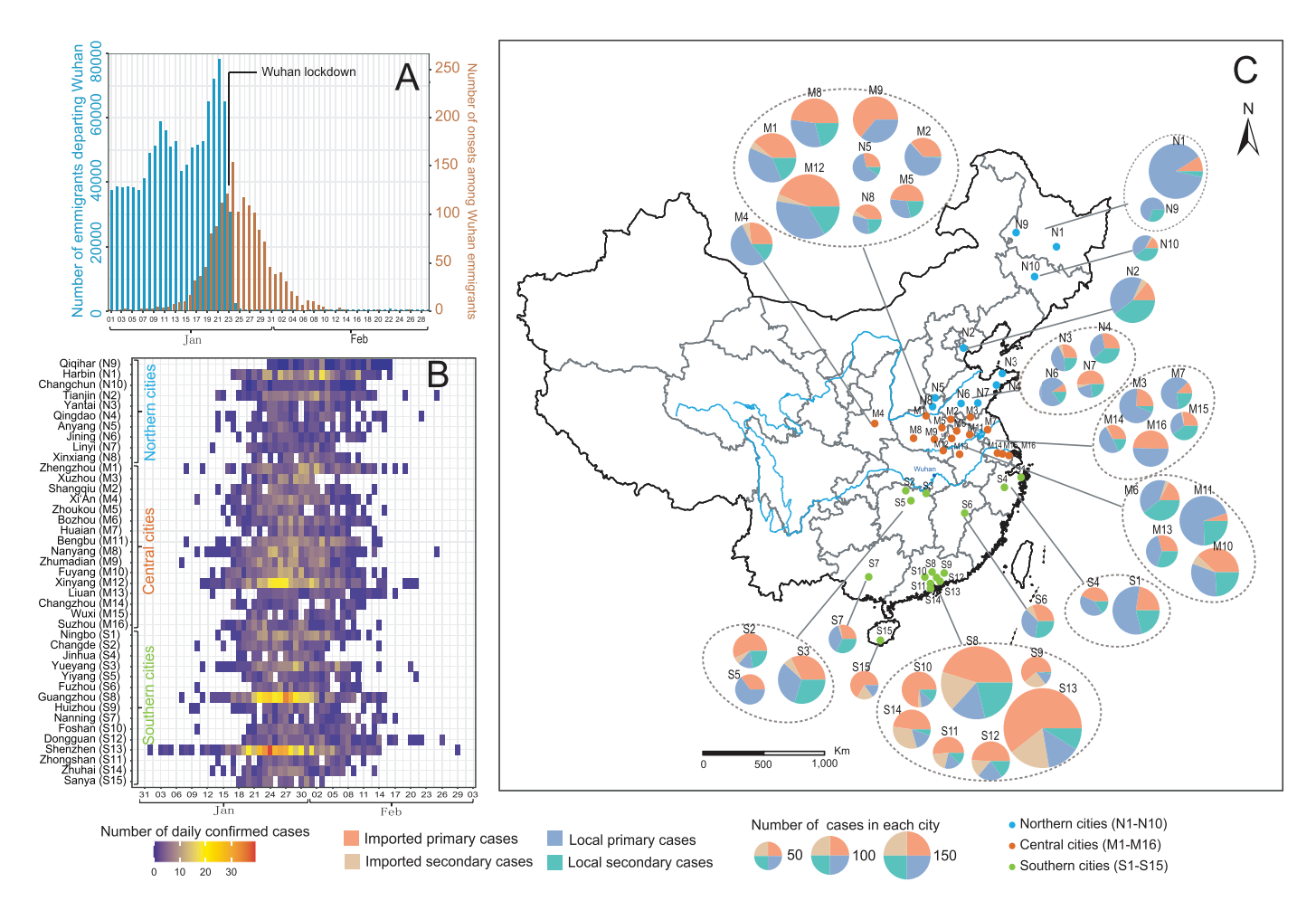


Fig. 1. Temporal and spatial distributions of COVID-19 cases in the crowdsourced contact-tracing data for the 41 cities of mainland China from January 1 to February 29, 2020. (A) Daily frequencies of emigrants departing Wuhan and symptom onsets of cases imported from Wuhan. (B) Daily numbers of symptom onsets among cases in each city. (C) Spatial distribution of the 41 cities and decomposition by case type in each city: imported primary, imported secondary, local primary and local secondary.

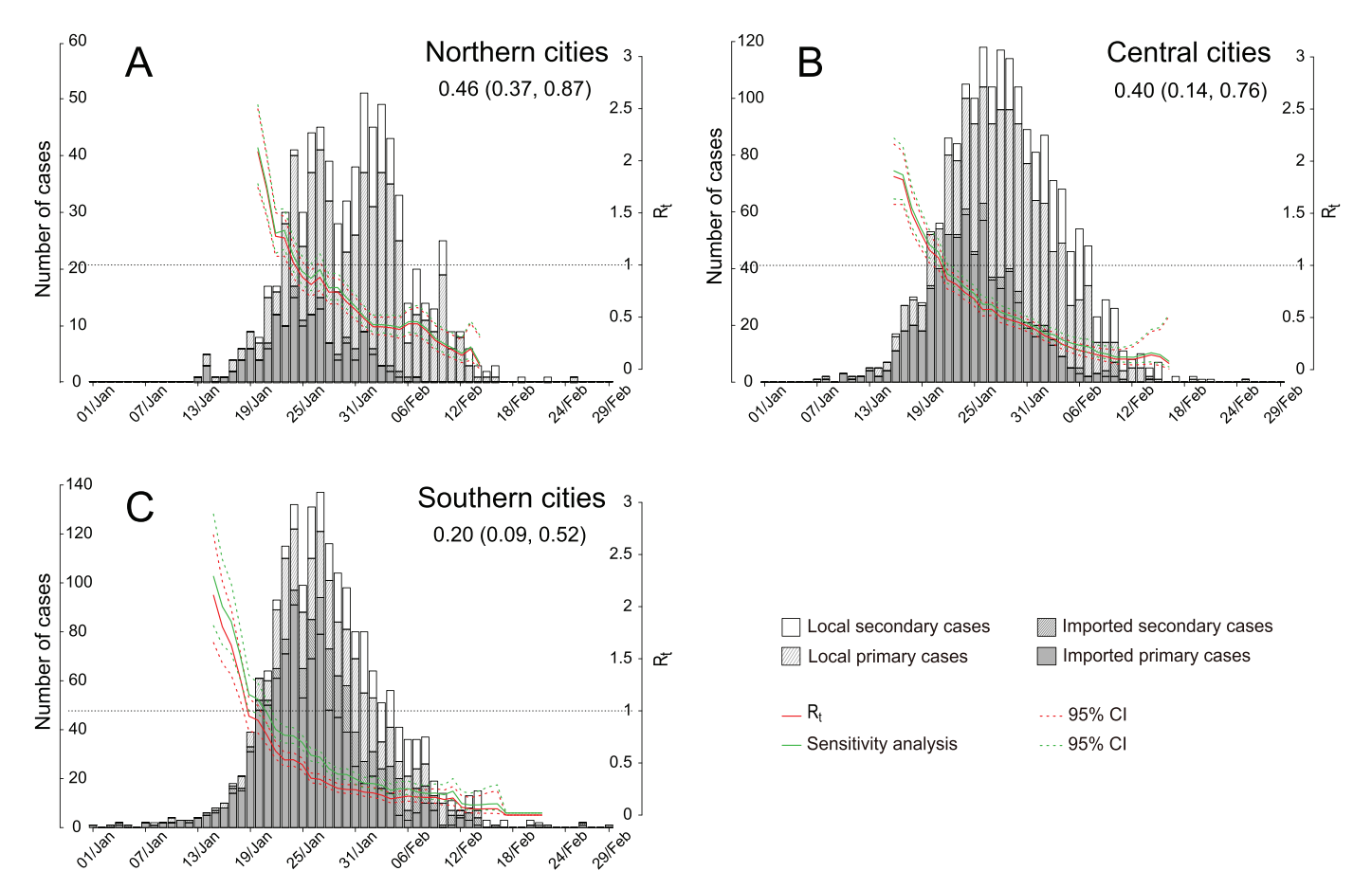


Fig. 2. Epidemic curves and estimated effective reproduction numbers (R_t) for (A) northern, (B) central and (C) southern China based on crowdsourced COVID-19 cases in 41 cities of mainland China from January 1 to February 29, 2020. Cases are classified into imported primary, imported secondary, local primary and local secondary and shaded correspondingly. R_t was estimated under two assumptions separately: imported secondary cases are considered as primary cases (infectors) in their clusters (red), and imported secondary cases are considered as secondary cases (infectors) in their clusters (green).

ern cities started with R_t below 1 (appendix p 16), compared to three out of ten northern cities (Appendix p 14), further suggesting higher transmissibility of COVID-19 in the north before the implementation of interventions.

Using GEE models, we found that temperature, relative humidity, immigration index, urban traffic index, and intervention measures jointly affected city-specific R_t values, whereas PM_{2.5} and population density did not (Appendix p 26). The best fit was obtained with time lags of 2, 3, 7 and 5 days for temperature, relative humidity, immigration index and urban traffic index, respectively. A higher R_t was associated with a lower temperature (Fig. 3A). The effect of relative humidity was not monotone. The local transmissibility of COVID-19 was low at both very low and very high levels of relative humidity and reached its peak at relative humidity near 75% (Fig. 3B). Both immigration index and urban transportation index were positively associated with R_t , indicating R_t was reduced by restrictions on intercity and intracity human movement (Fig. 3C-D). An increase of temperature from 0°C to 20°C would reduce the transmissibility by 30% (95 CI 10-46%), and a further increase to 30°C would reduce the transmissibility by another 17% (95% CI 5-27%) (Table 2). An increase of relative humidity from 40% to 75% would raise the transmissibility by 47% (95% CI 9-97%), but a further increase to 90% will moderately suppress the transmissibility by 12% (95% CI 4-19%). Decreases in the immigration index and urban traffic index from their median values before level-1 response to the median values after reduced the transmissibility by 5% (95% CI 1-9%) and 36% (95% CI 27-44%), respectively. As the level-1 response had very limited impact on the immigration

index (Appendix p 17), we assessed what would have happened had the human movement indices been decreased from their 75% percentiles to the 25% percentiles of the whole study period. Such changes in the immigration index or the urban traffic index would have reduced R_t by 8% and 45%, respectively. In addition to modulating R_t by reducing the human movement indices, the level-1 response further reduced R_t by 39% (95% CI 31–47%).

We performed sensitivity analysis by considering imported secondary cases as infectees rather than infectors. The estimated R_t values increased only moderately in a few southern cities with many visitors such as Guangzhou, Shenzhen and Sanya (Fig. 2; appendix p 14-16), and estimated effects of all the risk factors are robust to this change (Table 2, appendix p 27, Fig. 3, Appendix p 18). Fitting a GEE model to the expanded data set of 50 cities led to the drop-out of temperature but the addition of PM 2.5 (Appendix p 28); however, the risk ratio was moderately below 1 only at extremely large values of PM 2.5 and basically flat elsewhere (Appendix p 19). The effects of relative humidity, immigration index and urban traffic index were comparable to the primary results for the 41 cities (Appendix p 19 and 29). The effectiveness of the level-1 responses that were not related to human movement restriction, about 9%, was much smaller than 39% in the primary results (appendix p 29).

Finally, we predicted the R_t levels for the whole year of 2020. We first assume that, after Apr 27, 2020, human movement recovers to the average level before Chunyun (based on immigration and urban traffic indices during March of 2019), i.e., no human movement restriction, and level-1 emergency responses are

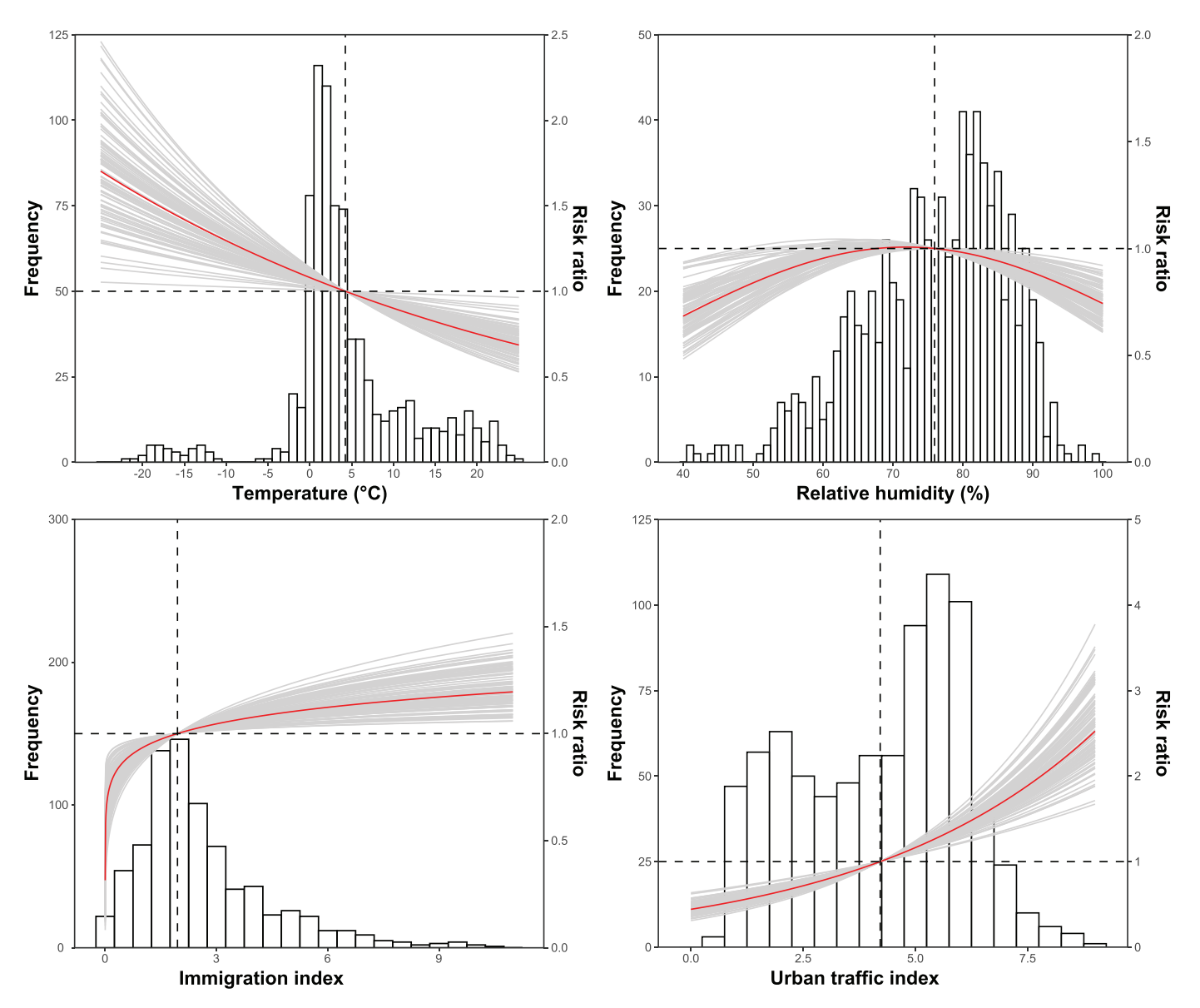


Fig. 3. Estimated risk-ratio curves (red) and observed frequencies (histogram) for (A) temperature, (B) relative humidity, (C) immigration index, and (D) urban traffic index on the effective reproduction number R_t based on a multivariable general estimation equation model fitted to daily R_t values in 41 cities of mainland China. Imported secondary cases were considered infectors for calculating R_t . The gray curves are the results of 100 times of parametric bootstrapping.

Table 2 Changes in mean R_t (risk ratio) between selected levels of independent variables, in the form of risk ratios (95% CI), based on the multivariable generalized estimated equation (GEE) applied to daily R_t values in the 41 cities of China.

Variable	Change [from, tol	Role of imported secondary Infector (Primary Analysis)	cases in calculating Rt Infectee (Sensitivity Analysis)
Temperature	[0, 20°C]	0•70 (0•54, 0•90)	0•74 (0•61, 0•91)
	[20°C, 30°C]	0.83 (0.73, 0.95)	0.86 (0.78, 0.96)
Relative	[40%, 75%]	1•47 (1•09, 1•97)	1•31 (0•98, 1•77)
humidity	[75%, 90%]	0.88 (0.81, 0.96)	0•92 (0•84, 0•99)
Level 1 response		0•61 (0•53, 0•69)	0•61 (0•53, 0•70)
Immigration	[2•41, 1•52]	0•95 (0•91, 0•99)	0•96 (0•93, 0•99)
index [†]	[3•32, 1•49]	0•92 (0•85, 0•99)	0•93 (0•87, 0•99)
Urban traffic	[5•50, 3•20]	0•64 (0•56, 0•83)	0.68 (0.60, 0.76)
index [‡]	[5•67, 2•56]	0•55 (0•46, 0•66)	0•59 (0•50, 0•70)

 $^{^\}dagger$ 2-41 and 1-52 are the median immigration index values before (including) and after 5 days post the initiation of level-1 response. 3-32 and 1-49 are the 75% and 25% percentiles of the immigration index.

 $^{^{\}ddagger}$ 5•50 and 3•20 are the median urban traffic index values before and after (including) the initiation of level-1 response. 5•67 and 2•56 are the 75% and 25% percentiles of the urban traffic index.

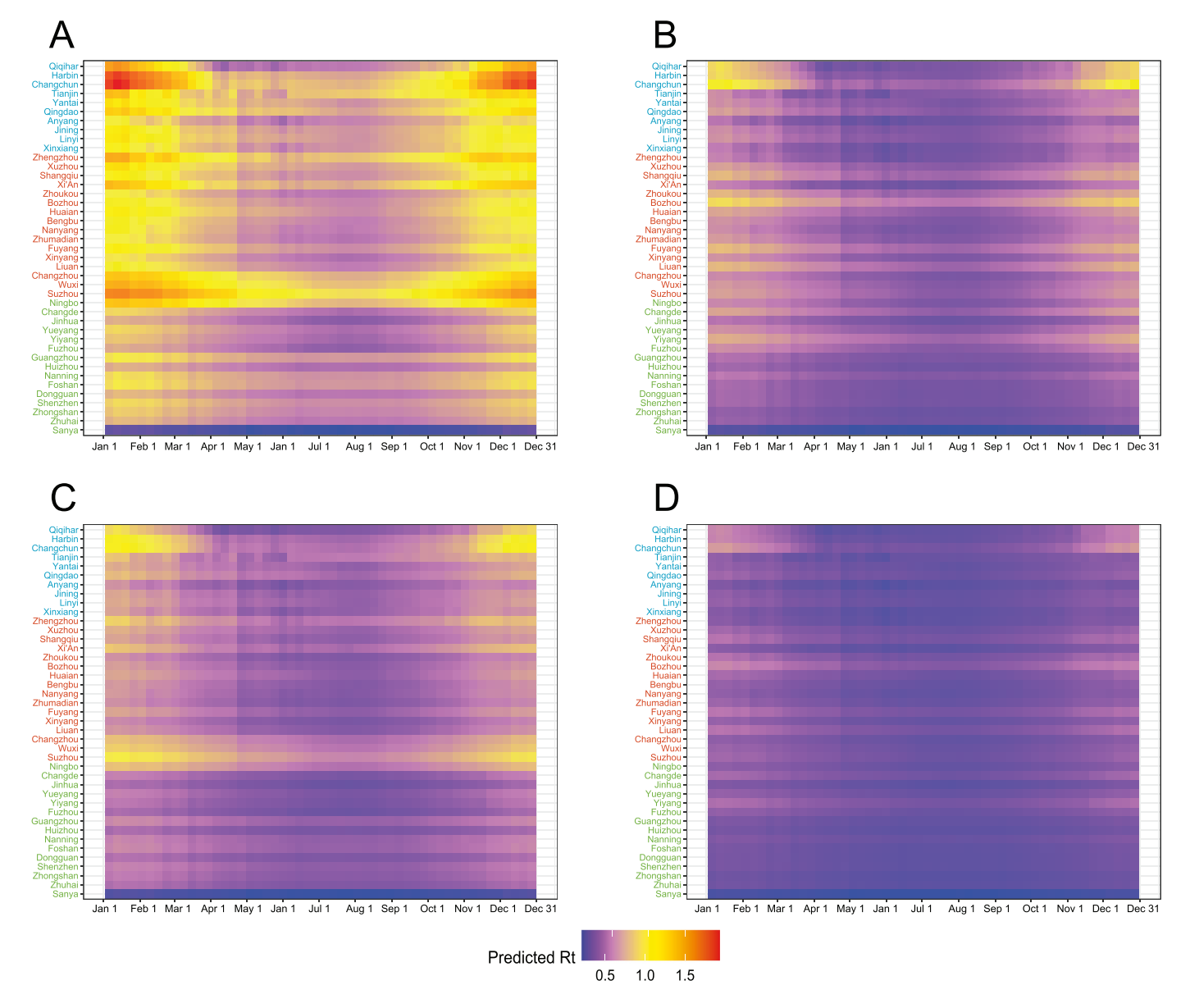


Fig. 4. Model-predicted weekly average R_t for 2020 under different assumptions about intervention policy: (A) level-1 emergency response is lifted, and human movement recovers to normal level, i.e., neither restricted nor within the spring festival commute period (immigration index and urban traffic index are set to the average level during March, 2019); (B) level-1 emergency response is lifted, but human movement is restricted (immigration index and urban traffic index are set to the average level during February, 2020); (C) level-1 emergency response is in place, but human movement recovers to normal level; and (D) Both level-1 emergency response and human movement restriction are in place.

absent after April (Fig. 4A). Rt remains below 1 from April to October in most cities but close to 1 in a few cities in northeastern China (Harbin and Changchun) or on the East Coast (Changzhou, Wuxi, Suzhou and Ningbo). The East Coast cities are popular destinations for tourists and migrant workers. By November, R_t reaches near or above 1.5 in Harbin, Changchun, Zhengzhou and Suzhou. In December and January, R_t increases to around 2 in Harbin and Changchun. Human movement restriction alone (Fig. 4B, based on immigration and urban traffic indices during Feb, 2020) or level-1 emergency response alone will bring R_t down to near or below 0.5 for most cities all the year round, although the former seems more effective than the latter. When level-1 emergency response is implemented alone, R_t remains close to 1 in Harbin, Changchun and Suzhou in the winter months (Fig. 4C). With human movement restriction and level-1 response both in place, R_t stays near or below 0.5 in all 41 cities throughout the year (Fig. 4D).

Discussion

Using a crowdsourced database, we characterized the distributions of the incubation period and serial interval of COVID-19 and assessed R_t values in 41 cities of China and associated drivers. The median R_t was higher in the northern cities than in the southern cities. We found COVID-19 was more locally transmissible at a low temperature and at a relative humidity near 75%. Both intracity and intercity human movements were driving factors for the transmissibility of COVID-19, but restricting intracity human movement was more effective. Other nonpharmaceutical interventions helped reducing R_t greatly. Our model-based prediction indicated potentially more active transmission in the northeastern region and the East Coast compared to other areas in China for the rest of the year, especially during the coming winter season, if human movement restrictions are lifted.

The estimated distribution of the incubation period is consistent with previous studies in which medians range from 5·1 to 6·4 days [18–20]. The longer incubation period post level-1 responses could be related to the increasing detection of mild cases. The estimates for the serial interval are also in line with estimates of 4–5 days by previous studies [18,21,22]. Faster detection of secondary cases post level-1 responses may explain the contraction of the serial interval over time.

Our estimation approach for R_t takes into account imported cases and clustering. The majority of existing estimates for R_t were based on a traditional method that does not distinguish between imported and local cases [15,23–24]. Other studies either adapted the traditional method or used transmission models to account for case importation, but those studies did not incorporate the clustering information [2,18]. Our estimates of R_t in Shenzhen resemble those in a modeling study but differ from another study which estimated an increasing trend of R_t before Jan 20 [2,18]. This difference could come from (1) whether R_t is attributed to the onset time of the infector (our study), and (2) the consideration of imported secondary cases as infectees (the previous study) or infectors (our study). Nevertheless, the overall subcritical levels of R_t in cities outside Hubei Province are consistent across most studies.

Our assessment of the effect of temperature on COVID-19 transmission is in consensus with many other studies [3,5]. While some studies found that transmission of SARS-CoV-2 and seasonal betacoronaviruses such as OC43 and HKU1was facilitated by lower relative or absolute humidity [6-7,25], others found this is not necessarily the case for SARS-CoV-2 [4,26]. Coronaviruses are wrapped by a lipid bilayer that makes it sustain longer in the air when relative humidity is low; on the other hand, a high relative humidity is associated with much longer survival on solid surfaces [27]. These two opposite effects of relative humidity on the survival of SARS-CoV-2 could partially explain our finding that a relative humidity near 75% maximizes local transmissibility of COVID-19. The first COVID-19 outbreak in a fresh (wet) seafood market in Wuhan and the recent outbreak in another seafood market in Beijing suggest the preference of the virus for cold and humid environments, consistent with our findings [28]. However, previous modeling studies suggested the epidemics in a dominantly susceptible population will not be decisively impacted by climatic determinants [7-8], which is also evidenced by the second wave of COVID-19 in southern United States during June, 2020 (https://coronavirus.jhu.edu/data/new-cases-50-states).

Both intercity and intracity human movements were important drivers for local transmission, but the latter (the urban traffic index) appeared more influential than the former (the immigration index). The mild yet statistically significant impact of intercity movement is likely due to different movement or contact patterns of visitors and tourists, compared to local residents. The level-1 emergency responses reduced intracity human movement to a much greater extent compared to intercity human movement (Appendix p 17), which is expected as intercity and interprovince commutes were not explicitly prohibited except for those to and from Wuhan. Even after adjusting for the human movement indices, the level-1 emergency responses further reduced R_t substantially, suggesting other control measures including but not limited to social distancing, case finding and isolation, contact tracing and quarantine, and mandatory mask-wearing had been effective in mitigating local transmission.

Our analyses bear several limitations. We have not considered the effect of changing definition of confirmed case by the Chinese Commission of Health and Family Planning during the epidemic of COVID-19, which could have led to artificial temporal patterns, e.g., a longer incubation period during the later epidemic phase as more milder and younger patients were detected [29].

Secondly, the study period for the association of R_t with climatic factors is relatively short, covering only January and February when air temperature was below 25°C in most cities of China. More data from the subsequent months and from other countries are needed to verify our findings. In addition, the subsets of cases contributing to the inference on the natural history of disease, R_t and associated determinants are all limited and may not fully represent the total of 11 003 cases in our database. These subsets share similar age and sex profiles with the whole database, but spatial-temporal distributions may differ (Appendix p 21). Furthermore, our database may not be representative of all cases in China; in particular, it lacks contact-tracing data from cities in Hubei Province, the epi-center in China. Consequently, our results could be subject to selection bias. Lastly, probable mutations in the viral genome could have contributed to the spatiotemporal variability in the local transmissibility of SARS-CoV-2, e.g., the recently reported "D614G" mutation in the S protein, which was not taken into account in our analyses [30].

The ideal environmental conditions against SARS-CoV-2, a high temperature plus either a very low or a very high relative humidity, may not be available or sustainable in many countries. South American countries such as Brazil, Peru and Chile are taking a hard hit by the ongoing pandemic of COVID-19 in their winter season. Meanwhile, parts of the United States are witnessing resurgence of local transmissions in their summer after shelter-at-home was lifted and social activities resumed. While classic control strategies including social distancing, timely case finding and isolation, and tracing and quarantine of close contacts can greatly reduce the transmissibility of COVID-19, it may be necessary to reactivate human movement restrictions to contain disease resurgence, especially when the climate is most suitable for viral transmission.

Research in context

Evidence before this study

On May 16, 2020, we searched PubMed, medRxiv and bioRxiv for all papers published in English from December 1, 2019 to May 16, 2020, using the search terms ("nCoV" OR "COVID" OR "novel coronavirus" OR "severe acute respiratory syndrome coronavirus 2") AND ("epidemiological characteristics" OR "transmission dynamics" OR "reproduction number" OR "meteorological factors" OR "nonpharmaceutical interventions"). We identified 95 relevant papers after screening.

Sixteen studies evaluated the effect of nonpharmaceutical interventions in mainland China. All these studies found the interventions to be effective, but very few directly assessed the effects solely due to human movement restrictions. One study found that social distancing led to a 7- to 8-fold reduction in contact rate based on survey and contact-tracing data from Wuhan, Shanghai and Hunan province. Three studies at the national scale found that banning intercity transportation after Wuhan lockdown had a limited effect on intercity spread, and two of them found that restricting intracity public transport greatly reduced case incidence.

About 19 of the 95 papers focused on the impact of meteorological factors but the findings are inconsistent. Five studies concluded that temperature had no impact, whereas 11 found a negative association between temperature and case incidence. One study indicated that a higher absolute humidity would benefit disease spread. Two studies found no impact of relative humidity on disease incidence, while four suggested a negative association. One study conducted in Brazilian cities found high temperatures and intermediate relative humidity are favorable conditions for the spread of COVID-19 in tropical climate.

Added value of this study

We assessed local transmissibility of COVID-19 in terms of the effective reproduction number (R_t) in 41 cities where our crowd-sourced data cover the dominant majority of reported cases (\geq 95% in 40 cities and 86% in one). Northern cities had noticeably higher R_t values than southern cities. By jointly considering meteorological variables, human movement indices and other nonpharmaceutical interventions in a statistical regression, we found low temperature and relative humidity in the range of 70–75% were ideal for the local transmission of COVID-19 in China. We found that restricting intracity transport alone reduced local transmissibility by 36% (95% CI 27–44%), but restricting intercity transport alone had limited effect. Nonpharmaceutical interventions other than human movement restrictions were also effective, reducing R_t by 39% (95% CI 31–47%). we predicted the potential R_t values in these cities throughout the year of 2020 under different levels of control.

Implications of all the available evidence

Temperature and relative humidity may potentially shape the seasonality of COVID-19 where the susceptible population are sufficiently depleted or effective interventions continue. While interventions such as social distancing, case finding and isolation, and tracing and quarantine of close contacts are efficient in inhibiting local transmission in most cities of China, they need to be used in conjunction with restriction of intracity human movement in central and northern China during the winter season to fully contain the disease.

Contributors

LQF, YY, and WL designed the study. HYZ, HZ, TLC, ARZ, MJL, WQS, JPG performed data sorting and database establishment. HYZ, HZ, TLC, ARZ, and MJL conducted the analyses under supervision of YY, YZ, WL and LQF. HYZ, LQF, YY and WL wrote the draft of the manuscript. All authors contributed to and approved the final version of the manuscript.

Data sharing statement

Deidentified data and R code used in the analyses can be downloaded as Multimedia Component 2.

Editor note: The Lancet Group takes a neutral position with respect to territorial claims in published maps and institutional affiliations.

Declaration of Competing Interest

We declare no competing interests.

Acknowledgment

This work was financially supported by grants from the China Mega-Project on Infectious Disease Prevention (No. 2018ZX10201001, 2018ZX10713001, 2018ZX10713002, and 2017ZX10303401), the National Natural Science Funds (No. 81825019), the U.S. National Institutes of Health (R01 Al139761 and R01 Al116770) and the U. S. National Science Foundation (2034364).

Supplementary materials

Supplementary material associated with this article can be found, in the online version, at doi:10.1016/j.lanwpc.2020.100020.

References

- Lai S, Ruktanonchai NW, Zhou L, et al. Effect of non-pharmaceutical interventions to contain COVID-19 in China. Nature 2020. doi:10.1038/ s41586-020-2293-x.
- [2] Leung K, Wu JT, Liu D, Leung GM. First-wave COVID-19 transmissibility and severity in China outside Hubei after control measures, and second-wave scenario planning: a modelling impact assessment. Lancet 2020;395:1382–93.
- [3] Tobías A, Molina T. Is temperature reducing the transmission of COVID-19. Environ Res 2020;186:109553.
- [4] Luo W, Majumder MS, Liu D, et al. The role of absolute humidity on transmission rates of the COVID-19 outbreak, medRxiv 2020; 2020.02.12.20022467.
- [5] Ujiie M, Tsuzuki S, Ohmagari N. Effect of temperature on the infectivity of COVID-19. Int | Infect Dis 2020;95:301–3.
- [6] Wang J, Tang K, Feng K, et al. High temperature and high humidity reduce the transmission of COVID-19. 2020. 10.2139/ssrn.3551767. (Accessed June 23, 2020)
- [7] Baker RE, Yang W, Vecchi GA, Metcalf CJE, Grenfell BT. Susceptible supply limits the role of climate in the early SARS-CoV-2 pandemic. Science 2020. doi:10.1126/science.abc2535.
- [8] Kissler SM, Tedijanto C, Goldstein E, Grad YH, Lipsitch M. Projecting the transmission dynamics of SARS-CoV-2 through the postpandemic period. Science 2020;368:860-8.
- [9] Viboud C, Bjørnstad ON, Smith DL, Simonsen L, Miller MA, Grenfell BT. Synchrony, waves, and spatial hierarchies in the spread of influenza. Science 2006;312:447–51.
- [10] Chinazzi M, Davis JT, Ajelli M, et al. The effect of travel restrictions on the spread of the 2019 novel coronavirus (COVID-19) outbreak. Science 2020;368:395–400.
- [11] Tian H, Liu Y, Li Y, et al. An investigation of transmission control measures during the first 50 days of the COVID-19 epidemic in China. Science 2020:368:638–42.
- [12] Zhang J, Litvinova M, Liang Y, et al. Changes in contact patterns shape the dynamics of the COVID-19 outbreak in China. Scienc 2020;368:1481–6.
- [13] Keeling MJ, Hollingworth TD, Read JM. Efficacy of contact tracing for the containment of the 2019 novel coronavirus (COVID-19). J Epidemiol Community Health 2020. doi:10.1136/jech-2020-214051.
- [14] Jing QL, Liu MJ, Zhang ZB, et al. Household secondary attack rate of COVID-19 and associated determinants in Guangzhou, China: a retrospective cohort study. Lancet Infect Dis 2020. doi:10.1016/S1473-3099(20)30471-0.
- [15] Wallinga J, Lipsitch M. How generation intervals shape the relationship between growth rates and reproductive numbers. Proc Biol Sci 2007;274:599-604.
- [16] Liang KY, Zeger SL. Longitudinal data analysis using generalized linear models. Biometrika 1986;73:13–22.
- [17] Pan W. Akaike's information criterion in generalized estimating equations. Biometrics 2001;57:120-5.
- [18] Zhang J, Litvinova M, Wang W, et al. Evolving epidemiology and transmission dynamics of coronavirus disease 2019 outside Hubei province, China: a descriptive and modelling study. Lancet Infect Dis 2020;20:793–802.
- [19] Linton NM, Kobayashi T, Yang Y, et al. Incubation period and other epidemiological characteristics of 2019 novel coronavirus infections with right truncation: a statistical analysis of publicly available case data. J Clin Med 2020;9:538.
- [20] Lauer SA, Grantz KH, Bi Q, et al. The incubation period of coronavirus disease 2019 (COVID-19) from publicly reported confirmed cases: estimation and application. Ann Intern Med 2020;172:577–82.
- pication. Ain intern Med 2020;172:577–82.

 [21] Nishiura H, Linton NM, Akhmetzhanov AR. Serial interval of novel coronavirus (COVID-19) infections. Int J Infect Dis 2020;93:284–6.
- [22] Du Z, Xu X, Wu Y, Wang L, Cowling BJ, Meyers LA. Serial interval of COVID-19 among publicly reported confirmed cases. Emerg Infect Dis 2020;26:1341–3.
- [23] Yuan J, Li M, Lv G, Lu ZK. Monitoring transmissibility and mortality of COVID-19 in Europe. Int J Infect Dis 2020;95:311–15.
- [24] You C, Deng Y, Hu W, et al. Estimation of the time-varying reproduction number of COVID-19 outbreak in China. Int J Hyg Environ Health 2020;228:113555.
- [25] Wu Y, Jing W, Liu J, et al. Effects of temperature and humidity on the daily new cases and new deaths of COVID-19 in 166 countries. Sci Total Environ 2020;729:139051.
- [26] Luo C, Yao L, Zhang L, et al. Possible transmission of severe acute respiratory syndrome coronavirus 2 (SARS-CoV-2) in a public bath center in Huai'an, Jiangsu Province, China. JAMA Network Open 2020;3:e204583.
- [27] Bhardwaj R, Agrawal A. Likelihood of survival of coronavirus in a respiratory droplet deposited on a solid surface. Phys Fluids 2020;32:061704.
- [28] Li Q, Guan X, Wu P, et al. Early transmission dynamics in Wuhan, China, of novel coronavirus-infected pneumonia. N Engl J Med 2020;382:1199–207.
- [29] Tsang TK, Wu P, Lin Y, Lau EHY, Leung GM, Cowling BJ. Effect of changing case definitions for COVID-19 on the epidemic curve and transmission parameters in mainland China: a modelling study. Lancet Public health 2020;5:e289–ee96.
- [30] Korber B, Fischer WM, Gnanakaran S, et al. Tracking changes in SARS-CoV-2 Spike: evidence that D614G increases infectivity of the COVID-19 virus. Cell 2020. doi:10.1016/j.cell.2020.06.043.